

U.S. Department of Commerce
National Oceanic and Atmospheric Administration
National Weather Service
National Centers for Environmental Prediction
5830 University Research Court
College Park, MD 20740

Office Note 474

Comparative computational efficiency of stencils suitable for the estimation of horizontal Taylor expansion coefficients

R. James Purser*
IM Systems Group, Rockville, Maryland

November 26, 2013

THIS IS AN UNREVIEWED MANUSCRIPT, PRIMARILY INTENDED FOR INFORMAL
EXCHANGE OF INFORMATION AMONG THE NCEP STAFF MEMBERS

* email: jim.purser@noaa.gov

Abstract

Observation forward operators for many remotely-sensed data used in the assimilation for numerical weather prediction have a “footprint” of horizontal extent sufficiently large to warrant a better representation than the simple “point-like” representation currently applied. This is especially true of Global Positioning System radio occultation data and limb sounders. But even vertical passive sounders also possess horizontal footprints whose sizes can exceed the grid spacing of typical modern weather prediction models. One approach to achieving a better handling of such data is to integrate their characteristic footprint weight functions over a polynomial fitted to the local horizontal distribution of the variable to which the measurement instrument is sensitive, at each relevant vertical level. The viability of such an approach depends upon the acquisition of the fitted polynomial’s coefficients in a computationally efficient way. This brief note examines a selection of plausible choices of stencils from a regular lattice that can serve as the source data for the extraction of the needed coefficients and attempts to provide guidance towards optimal choices at each order of expansion based on minimizing the computational cost.

1. INTRODUCTION

In an earlier office note (Purser 2007) we introduced efficient methods for interpolating a point value, or the gradient of that value, from a two- or three-dimensional lattice, based on the use of “diamond” stencils which minimized the computational cost while promoting a high level of accuracy given the order of the accuracy required. The basic diamond stencil at a given order of accuracy consists of exactly as many points as there are Taylor expansion coefficients needed to construct the interpolated value to the desired order. But if the objective is to acquire this entire set of expansion coefficients (not just the inferred interpolated value at some given target point), then the basic diamond stencil, owing to its relatively low degree of symmetry compared to other slightly larger stencils, is not necessarily optimal in terms of the count of arithmetic operations needed to secure the result. Also, in order to optimize the use of the basic diamond stencil, and its more symmetric but slightly larger modifications, for the purpose of extracting the expansion coefficients, whatever symmetries each of the stencils possesses should be exploited. In addition, there are some non-obvious empirical linear transformations of the first few of the basic two-dimensional diamond stencils’ values, reflecting partial symmetries or simply numerical coincidences, which enhance their efficiency beyond that achieved using only their obvious bilateral symmetry.

2. DIAMOND STENCILS

We shall concern ourselves only with two-dimensional stencils here. In those cases where the (Taylor) expansion coefficients of the fitted polynomial are destined to be used in a horizontal integration with some “footprint” function that is invariant with respect to vertical level, then the integration weights associated with the stencil points is similarly invariant with respect to vertical level.

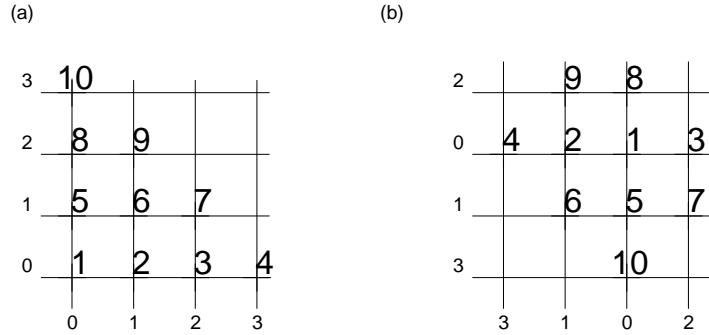


Figure 1. Construction of standard “diamond” stencil (b) from a logical triangular stencil (a) of the same number of points

Figure 1 illustrates the construction of the basic diamond stencil and its logical equivalence to the triangular stencil. Associated with each of the triangular stencil points (and therefore, with each of the diamond stencil points) is a particular term of fitted polynomial. For example, the point with x and y coordinate labels i and j , where $0 \leq i$, $0 \leq j$ and $i + j \leq m$ for the polynomial degree m is associated with the term in the polynomial with powers of x and y , $x^i y^j$, in the sense explained as follows. In order to fit the polynomial to the given triangular stencil values we can run down the outer diagonal ($i + j = m$) of coefficients and evaluate each one of them unambiguously, using only the rectangle of stencil data for which the indices are i' , j' , with $i' \leq i$ and $j' \leq j$. This i, j coefficient is obtained simply as the cartesian product of the degree- i derivative in x and the degree- j derivative in y , within this sub-rectangle of the larger stencil. Then we discard the i, j stencil member and subtract this diagnosed $x^i y^j$ term from all the remaining stencil members. Continuing in this way until all the outer-diagonal stencil members have been used up, we continue the same process for the diminished triangular stencil, systematically exhausting *its* outer diagonal of elements i, j for which $i + j = m - 1$, and so on. This procedure does not depend on the coordinates x_i being uniform, or even monotonic in x ; just as long as they are distinct. Similarly for the y_j coordinates of the stencil points. So the procedure will formally work with the approximately diamond-shaped stencil of Fig. 1(b), where the labels of the lines of the stencil alternate according to:

$$x_i = \begin{cases} i/2 & : & i & \text{even} \\ -(i+1)/2 & : & i & \text{odd} \end{cases} \quad (2.1)$$

and similarly for y_i . Also, this step-by-step exhaustive procedure for estimating the Taylor coefficients will still work even if the original stencil's i and j bounds do not form a tidy diagonal pattern, provided the maximum j at each i is a nonincreasing function of the i , and vice-versa, and the lines in the stencil display no gaps. Thus, the logical stencil shown in Fig. 2(a) is also valid for evaluating the corresponding stencil of Taylor coefficients, but the stencil in Fig. 2(b) is not (nonmonotonicity of its boundary, and gaps).

These considerations restrict the ways we are permitted to augment the basic diamond stencils if we want to obtain modifications that possess additional symmetries. The only sym-



Figure 2. (a) A logical stencil arrangement from which it is possible to apply the sequential procedure to extract Taylor coefficients without ambiguity. (b) A non-monotonic stencil for which the sequential procedure will not work.

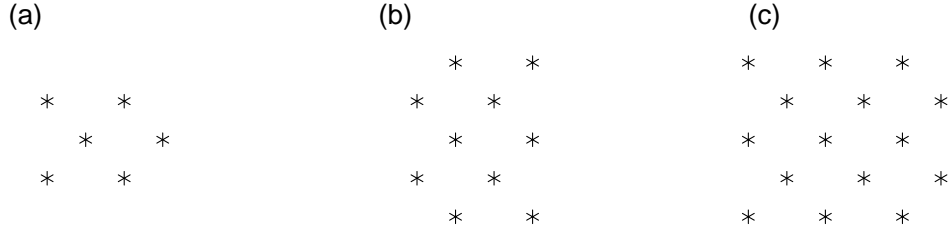


Figure 3. Standard diamond interpolation stencils, but rotated to place the axis of bilateral symmetry parallel to the x -coordinate direction. (a) 2nd-order stencil of six points; (b) 3rd-order stencil of 10 points; (c) 4th-order stencil of 15 points.

metry possessed by the basic diamond stencils is the bilateral symmetry they all share. In the example shown in Fig. 1(b), this symmetry's axis is the 45-degree diagonal through the origin. It convenient to rotate the cartesian coordinate system, (x, y) , to make this the x -axis. The stencils (a), (b), (c) depicted in Fig. 3 are the standard diamond stencils capable of providing Taylor series of orders $m = 2, 3$ and 4 respectively.

(a) *Examples of efficient schemes for the standard diamond stencils*

In the orientation of Fig. 3 we can take the stencil locations to have coordinates that are pairs of integers that sum to an even value. From the six sampled values $P_{i,j}$ for the 2nd order stencil of Fig. 3(a) we can form symmetric and antisymmetric off-axis combinations by additions and subtractions:

$$\begin{aligned}
 P_{-1,1}^+ &= P_{-1,1} + P_{-1,-1}, \\
 P_{1,1}^+ &= P_{1,1} + P_{1,-1}, \\
 P_{-1,1}^- &= P_{-1,1} - P_{-1,-1}, \\
 P_{1,1}^- &= P_{1,1} - P_{1,-1}.
 \end{aligned}$$

A further set of adding and subtracting transformations of the symmetric (including on-axis) quantities to:

$$\begin{aligned}
 \overline{P}_{0,0}^+ &= P_{0,0}, \\
 \overline{P}_{1,0}^+ &= -P_{0,0} + P_{1,0}, \\
 \overline{P}_{0,1}^+ &= P_{-1,1}^+ + P_{1,1}^+, \\
 \overline{P}_{1,1}^+ &= -P_{-1,1}^+ + P_{1,1}^+,
 \end{aligned} \tag{2.2}$$

and the antisymmetric quantities to:

$$\begin{aligned}\overline{P}_{0,1}^- &= P_{-1,1}^- + P_{1,1}^-, \\ \overline{P}_{1,1}^- &= -P_{-1,1}^- + P_{1,1}^-, \end{aligned} \quad (2.3)$$

enables the complete set of six Taylor expansion coefficients up to second degree to be obtained very economically:

$$C_{0,0} = \overline{P}_{0,0}^+ \equiv P_{0,0}, \quad (2.4a)$$

$$C_{1,0} = \frac{1}{4}\overline{P}_{1,1}^+, \quad (2.4b)$$

$$C_{2,0} = \frac{1}{2}\overline{P}_{1,0}^+ - C_{1,0}, \quad (2.4c)$$

$$C_{0,2} = -C_{2,0} - 2\overline{P}_{0,0}^+ + \frac{1}{2}\overline{P}_{0,1}^+, \quad (2.4d)$$

$$C_{0,1} = \frac{1}{4}\overline{P}_{0,1}^-, \quad (2.4e)$$

$$C_{1,1} = \frac{1}{4}\overline{P}_{1,1}^-. \quad (2.4f)$$

Here, $C_{i,j}$ represents the approximated derivative at the origin,

$$C_{i,j} = \frac{\partial^{i+j} P}{\partial x^i \partial y^j}, \quad (2.5)$$

(zeroth derivative meaning the value itself, of course). Note that this sequence of arithmetic operations is significantly more efficient than the more straight-forward alternative of deriving the six Taylor coefficients from the six stencil values via a matrix-vector multiply.

In examples of higher order Taylor series evaluations, it *is* helpful to use matrices to express some of the the necessary linear transformations of an efficient sequence, but in these cases we expect the matrices to be significantly sparse. For one example, the 3rd-order stencil of Fig. 3(b) can be converted into its off-axis symmetric (P^+) and antisymmetric (P^-) combinations and the Taylor coefficient estimates with positive and negative symmetry obtained directly from them according to the pair of matrix equations:

$$\begin{bmatrix} C_{0,0} \\ C_{1,0} \\ C_{2,0} \\ C_{3,0} \\ \hline C_{0,2} \\ C_{1,2} \end{bmatrix} = \begin{bmatrix} 1 & 0 & 0 & 0 & 0 & 0 \\ -\frac{1}{2} & 0 & -\frac{1}{6} & \frac{1}{2} & 0 & -\frac{1}{12} \\ -\frac{3}{2} & 0 & \frac{1}{2} & \frac{1}{2} & -\frac{1}{4} & 0 \\ \frac{9}{4} & \frac{3}{4} & -\frac{1}{2} & -\frac{3}{2} & \frac{3}{8} & \frac{1}{8} \\ \hline -\frac{1}{2} & 0 & 0 & 0 & \frac{1}{4} & 0 \\ \frac{1}{4} & -\frac{1}{4} & 0 & 0 & -\frac{1}{8} & \frac{1}{8} \end{bmatrix} \begin{bmatrix} P_{0,0} \\ P_{2,0} \\ \hline P_{-1,1}^+ \\ P_{1,1}^+ \\ \hline P_{0,2}^+ \\ P_{2,2}^+ \end{bmatrix}, \quad (2.6)$$

and

$$\begin{bmatrix} C_{0,1} \\ C_{1,1} \\ C_{2,1} \\ \text{---} \\ C_{0,3} \end{bmatrix} = \begin{bmatrix} \frac{1}{6} & \frac{1}{2} & 0 & -\frac{1}{12} \\ -\frac{1}{4} & \frac{1}{4} & 0 & 0 \\ \frac{1}{4} & -\frac{1}{4} & -\frac{1}{8} & \frac{1}{8} \\ \text{---} & \text{---} & \text{---} & \text{---} \\ -\frac{1}{4} & -\frac{3}{4} & \frac{3}{8} & \frac{1}{8} \end{bmatrix} \begin{bmatrix} P_{-1,1}^- \\ P_{1,1}^- \\ \text{---} \\ P_{0,2}^- \\ P_{2,2}^- \end{bmatrix}. \quad (2.7)$$

A crude estimate of the computational cost involved in acquiring these Taylor coefficients comes from summing the number of “multiply” operations involved (i.e., we ignore sums and differences). Thus the nominal cost for the 3rd-order Taylor coefficients by this scheme amounts to 34 units by this measure. To obtain a very modest gain that reduces this measure to just 30 units, an alternative calculation involving the linear combinations:

$$\overline{P}_{0,0}^+ = P_{0,0}, \quad (2.8a)$$

$$\overline{P}_{1,0}^+ = -P_{0,0} + P_{2,0}, \quad (2.8b)$$

$$\overline{P}_{0,1}^+ = P_{-1,1}^+ + P_{1,1}^+, \quad (2.8c)$$

$$\overline{P}_{1,1}^+ = -P_{-1,1}^+ + P_{1,1}^+, \quad (2.8d)$$

$$\overline{P}_{0,2}^+ = P_{0,2}^+, \quad (2.8e)$$

$$\overline{P}_{1,2}^+ = -P_{0,2}^+ + P_{2,2}^+, \quad (2.8f)$$

and:

$$\overline{P}_{0,1}^- = P_{-1,1}^- + P_{1,1}^-, \quad (2.9a)$$

$$\overline{P}_{1,1}^- = -P_{-1,1}^- + P_{1,1}^-, \quad (2.9b)$$

$$\overline{P}_{0,2}^- = P_{0,2}^-, \quad (2.9c)$$

$$\overline{P}_{1,2}^- = -P_{0,2}^- + P_{2,2}^-, \quad (2.9d)$$

can be used to construct the same coefficient vectors:

$$\begin{bmatrix} C_{0,0} \\ C_{1,0} \\ C_{2,0} \\ C_{3,0} \\ \text{---} \\ C_{0,2} \\ C_{1,2} \end{bmatrix} = \begin{bmatrix} 1 & 0 & 0 & 0 & 0 & 0 \\ -\frac{1}{2} & 0 & \frac{1}{6} & \frac{1}{3} & -\frac{1}{12} & -\frac{1}{12} \\ -\frac{3}{2} & 0 & \frac{1}{2} & 0 & -\frac{1}{4} & 0 \\ 3 & \frac{3}{4} & -1 & -\frac{1}{2} & \frac{1}{2} & \frac{1}{8} \\ \text{---} & \text{---} & \text{---} & \text{---} & \text{---} & \text{---} \\ -\frac{1}{2} & 0 & 0 & 0 & \frac{1}{4} & 0 \\ 0 & -\frac{1}{4} & 0 & 0 & 0 & \frac{1}{8} \end{bmatrix} \begin{bmatrix} \overline{P}_{0,0}^+ \\ \overline{P}_{1,0}^+ \\ \text{---} \\ \overline{P}_{0,1}^+ \\ \overline{P}_{1,1}^+ \\ \text{---} \\ \overline{P}_{0,2}^+ \\ \overline{P}_{1,2}^+ \end{bmatrix}, \quad (2.10)$$

and

$$\begin{bmatrix} C_{0,1} \\ C_{1,1} \\ C_{2,1} \\ \text{---} \\ C_{0,3} \end{bmatrix} = \begin{bmatrix} \frac{1}{3} & \frac{1}{6} & -\frac{1}{12} & -\frac{1}{12} \\ 0 & \frac{1}{4} & 0 & 0 \\ 0 & -\frac{1}{4} & 0 & \frac{1}{8} \\ \text{---} & \text{---} & \text{---} & \text{---} \\ -\frac{1}{2} & -\frac{1}{4} & \frac{1}{2} & \frac{1}{8} \end{bmatrix} \begin{bmatrix} \overline{P}_{0,1}^- \\ \overline{P}_{1,1}^- \\ \text{---} \\ \overline{P}_{0,2}^- \\ \overline{P}_{1,2}^- \end{bmatrix}. \quad (2.11)$$

For another example, the 4th order diamond stencil of Fig. 3(c) can be converted into its off-axis symmetric (P^+) and antisymmetric (P^-) combinations as before, by sums and differences, and these can be further manipulated to form the intermediate vectors with components:

$$\overline{P}_{0,0}^+ = P_{0,0}, \quad (2.12a)$$

$$\overline{P}_{1,0}^+ = -P_{2,0} + P_{2,0}, \quad (2.12b)$$

$$\overline{P}_{2,0}^+ = P_{-2,0} - 6P_{0,0} + 5P_{2,0}, \quad (2.12c)$$

$$\overline{P}_{0,1}^+ = 5P_{-1,1}^+ + 10P_{1,1}^+ + P_{3,1}^+, \quad (2.12d)$$

$$\overline{P}_{1,1}^+ = -P_{-1,1}^+ + P_{1,1}^+, \quad (2.12e)$$

$$\overline{P}_{2,1}^+ = -3P_{-1,1}^+ + 2P_{1,1}^+ + P_{3,1}^+, \quad (2.12f)$$

$$\overline{P}_{0,2}^+ = P_{-2,2}^+ - 2P_{0,2}^+ + 5P_{2,2}^+, \quad (2.12g)$$

$$\overline{P}_{1,2}^+ = -P_{-2,2}^+ + P_{2,2}^+, \quad (2.12h)$$

$$\overline{P}_{2,2}^+ = -P_{-2,2}^+ - 2P_{0,2}^+ + 3P_{2,2}^+, \quad (2.12i)$$

$$\overline{P}_{0,1}^- = P_{-1,1}^- + P_{1,1}^-, \quad (2.13a)$$

$$\overline{P}_{1,1}^- = -P_{-1,1}^- + P_{1,1}^-, \quad (2.13b)$$

$$\overline{P}_{2,1}^- = P_{-1,1}^- - 2P_{1,1}^- + 3P_{3,1}^-, \quad (2.13c)$$

$$\overline{P}_{0,2}^- = P_{-2,2}^- + P_{2,2}^-, \quad (2.13d)$$

$$\overline{P}_{1,2}^- = -P_{-2,2}^- + P_{2,2}^-, \quad (2.13e)$$

$$\overline{P}_{2,2}^- = P_{-2,2}^- - 2P_{0,2}^- + P_{2,2}^-, \quad (2.13f)$$

and the final pair of transformations are, again, most easily written in sparse matrix terms. For

the symmetric terms we find:

$$\begin{bmatrix} C_{0,0} \\ C_{1,0} \\ C_{2,0} \\ C_{3,0} \\ C_{4,0} \\ \text{---} \\ C_{0,2} \\ C_{1,2} \\ C_{2,2} \\ \text{---} \\ C_{0,4} \end{bmatrix} = \begin{bmatrix} 1 & 0 & 0 & 0 & 0 & 0 & 0 & 0 & 0 \\ 0 & 0 & 0 & 0 & \frac{1}{3} & 0 & 0 & -\frac{1}{24} & 0 \\ 0 & 0 & \frac{1}{8} & 0 & 0 & -\frac{1}{12} & 0 & 0 & \frac{1}{48} \\ 0 & \frac{3}{8} & 0 & 0 & -\frac{1}{2} & 0 & 0 & \frac{1}{16} & 0 \\ 0 & -\frac{1}{2} & -\frac{1}{8} & 0 & 0 & \frac{1}{4} & 0 & 0 & -\frac{1}{16} \\ \text{---} & \text{---} \\ -\frac{5}{2} & 0 & -\frac{1}{8} & \frac{1}{12} & 0 & 0 & -\frac{1}{48} & 0 & 0 \\ 0 & -\frac{1}{8} & 0 & 0 & 0 & 0 & 0 & \frac{1}{16} & 0 \\ 0 & \frac{1}{12} & -\frac{1}{24} & 0 & 0 & 0 & 0 & -\frac{1}{8} & \frac{1}{16} \\ \text{---} & \text{---} \\ 6 & 0 & \frac{3}{8} & -\frac{1}{4} & 0 & 0 & \frac{1}{4} & \frac{3}{4} & \frac{9}{16} \end{bmatrix} \begin{bmatrix} \overline{P}_{0,0}^+ \\ \overline{P}_{1,0}^+ \\ \overline{P}_{2,0}^+ \\ \text{---} \\ \overline{P}_{0,1}^+ \\ \overline{P}_{1,1}^+ \\ \overline{P}_{2,1}^+ \\ \text{---} \\ \overline{P}_{0,2}^+ \\ \overline{P}_{1,2}^+ \\ \overline{P}_{2,2}^+ \end{bmatrix}, \quad (2.14)$$

and for the antisymmetric terms we find:

$$\begin{bmatrix} C_{0,1} \\ C_{1,1} \\ C_{2,1} \\ C_{3,1} \\ \text{---} \\ C_{0,3} \\ C_{1,3} \end{bmatrix} = \begin{bmatrix} \frac{1}{3} & 0 & 0 & -\frac{1}{24} & 0 & 0 \\ 0 & \frac{1}{3} & 0 & 0 & -\frac{1}{48} & 0 \\ 0 & 0 & 0 & 0 & 0 & \frac{1}{16} \\ 0 & 0 & \frac{1}{8} & 0 & 0 & -\frac{1}{16} \\ \text{---} & \text{---} & \text{---} & \text{---} & \text{---} & \text{---} \\ -\frac{1}{2} & 0 & 0 & \frac{1}{4} & 0 & -\frac{3}{16} \\ 0 & -\frac{1}{2} & -\frac{1}{8} & 0 & \frac{1}{8} & \frac{1}{16} \end{bmatrix} \begin{bmatrix} \overline{P}_{0,1}^- \\ \overline{P}_{1,1}^- \\ \overline{P}_{2,1}^- \\ \text{---} \\ \overline{P}_{0,2}^- \\ \overline{P}_{1,2}^- \\ \overline{P}_{2,2}^- \end{bmatrix}. \quad (2.15)$$

In this case, the cost of preparing the intermediate vectors \overline{P}^+ and \overline{P}^- should be included since 13 nontrivial multiplies are involved in this step, Combining these with the 43 nonzero elements of the matrices in (2.14) and (2.15) we set a nominal measure of cost as 56 units for this 4th-order scheme.

The combinations used to obtain the \overline{P}^\pm were, in the 3rd and 4th-order cases, chosen empirically, but to examine schemes of higher order we would need a more systematic approach to generalizing this kind of pre-conditioning step. The sizes of the stencils of the higher order schemes for the standard diamond and for various symmetrized (but unrotated) versions of these stencils (described in the next section) are listed in Table 2, together with the sizes of the square stencils obtained simply by taking the cartesian products of one-dimensional centered stencils. We shall not delve into details for the higher order schemes since, for the standard diamond stencils, the results remain inferior in computational economy to the competing symmetrized-stencils we consider in the next section. Suffice it to say that the best general preconditioning

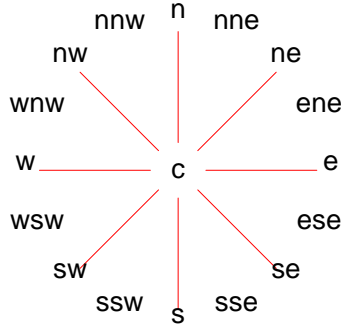


Figure 4. Schematic definition of the 17 “sectors” into which we divide the points of a symmetrized stencil. Sector “c” is the central point by itself (if it belongs to the stencil); sectors “e”, “ne”, “n”, “nw”, “w”, “sw”, “s” and “se” are the degenerate sectors comprising the radial lines indicated; sectors “ese”, “nne”, “nnw”, “wnw”, “wsw”, “ssw”, “sse” are the interleaved true sectors spanning the designated 45 degree wedges, excluding their bounding angles.

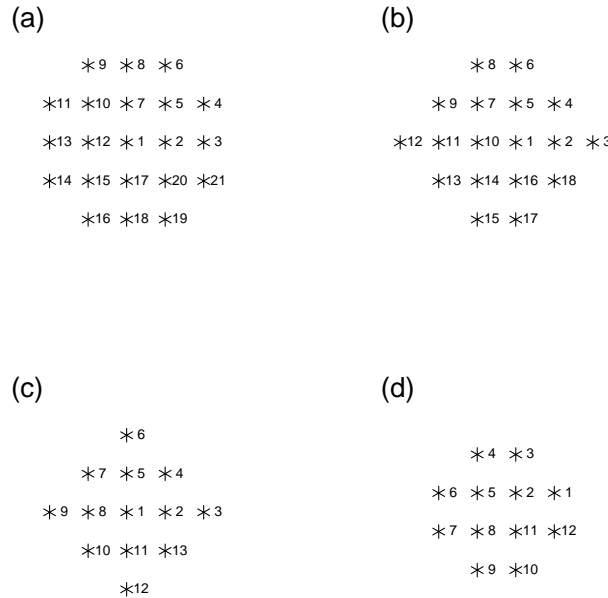


Figure 5. Unrotated diamond interpolation stencils augmented to gain higher degrees of symmetry under reflection. (a) Type “T” of 4th-order; (b) Type “U” of 4th-order; (c) Type “V” of 3rd-order; (d) Type “W” of 3rd-order

strategy we have found has been, as in the 3rd-order case, to apply to each x-line and to each y-line of the given stencil, a transformation from the values along the lines to the first few finite derivatives along the lines, computed to the highest order that the length of each line allows, and centered at the intended coordinate origin for the final Taylor series. When this is done the nominal computational costs, estimated exactly as before, are the values listed in the column “S” of the Table 3. The other entries in this table refer to the costs for the various symmetrized augmentations of the diamond stencil, or to the logically simplest, but often most costly scheme, the Cartesian product scheme, all of which we describe next.

TABLE 1. ACTION OF THE OPERATORS, F , G , AND H , ON THE SUBVECTORS, ARRANGED BY DIRECTIONAL SECTORS, OF THE FULL STENCIL VECTOR P . THE SUFFICES OF THE SUBVECTORS INDICATE THE SECTOR BY ITS ASSOCIATED COMPASS DIRECTION.

Result	F	G	H
P'_c	P_c	P_c	P_c
P'_e	P_e	$P_e + P_w$	$P_e + P_n$
P'_{ene}	$P_{ene} + P_{ese}$	$P_{ene} + P_{wnw}$	$P_{ene} + P_{nne}$
P'_{ne}	$P_{ne} + P_{se}$	$P_{ne} + P_{nw}$	P_{ne}
P'_{nne}	$P_{nne} + P_{sse}$	$P_{nne} + P_{nnw}$	$P_{ene} - P_{nne}$
P'_n	$P_n + P_s$	P_n	$P_e - P_n$
P'_{nnw}	$P_{nnw} + P_{ssw}$	$P_{nne} - P_{nnw}$	$P_{ese} + P_{nnw}$
P'_{nw}	$P_{nw} + P_{sw}$	$P_{ne} - P_{nw}$	$P_{se} + P_{nw}$
P'_{wnw}	$P_{wnw} + P_{wsw}$	$P_{ene} - P_{wnw}$	$P_{sse} + P_{wnw}$
P'_w	P_w	$P_e - P_w$	$P_s + P_w$
P'_{wsw}	$P_{wnw} - P_{wsw}$	$P_{ese} - P_{wsw}$	$P_{ssw} + P_{wsw}$
P'_{sw}	$P_{nw} - P_{sw}$	$P_{se} - P_{sw}$	P_{sw}
P'_{ssw}	$P_{nnw} - P_{ssw}$	$P_{sse} - P_{ssw}$	$P_{ssw} - P_{wsw}$
P'_s	$P_n - P_s$	P_s	$P_s - P_w$
P'_{sse}	$P_{nne} - P_{sse}$	$P_{sse} + P_{ssw}$	$P_{sse} - P_{wnw}$
P'_{se}	$P_{ne} - P_{se}$	$P_{se} + P_{sw}$	$P_{se} - P_{nw}$
P'_{ese}	$P_{ene} - P_{ese}$	$P_{ese} + P_{wsw}$	$P_{ese} - P_{nnw}$

3. SYMMETRIZED STENCIL SCHEMES

For the symmetrized stencils, it is convenient to organize their sampled values, and the Taylor coefficients that correspond with their locations, into subvectors associated with the distinct sectors around the center of symmetry. The first, sector “c” denotes the central point itself (if it belongs to the stencil). The 16 sectors that follow it are indexed according to compass directions starting for with “e” (east) and incrementing in the counterclockwise direction, “e”, “ene”, “ne”, “nne”, etc., as illustrated in Fig. 4. The sectors alternate between sets of points that lie along radial lines (“e”, “ne” etc.) and true geometrical sectors (“ene”, “nne”, etc) of points that lie strictly between those radial lines. Various symmetric and antisymmetric combinations of the stencil values can be computed by operations of addition and subtraction, summarized in Table 1 and denoted the linear operators: F (reflection symmetry/antisymmetry about the east-west axis); G (reflection symmetry/antisymmetry about the north-south axis); H (reflection symmetry/antisymmetry about the line ne—sw). We shall assume that, within a radial line sector (such as “e”) the points are listed in order of increasing radius; within a true sector (such as “ene”) we assume the points are listed in rows parallel to the neighboring cardinal direction, with the rows listed in order of distance from the associated cartesian axis. The application of the symmetrizing operators, F , G and H serves to simplify the remaining linear operator step, M , between stencil values and their implied polynomial-fitted Taylor

coefficients by rendering \mathbf{M} effectively block diagonal and hence, relatively sparse. The benefits of the H operator are only obtained when it is applied immediately before and after \mathbf{M} itself, and as H^T at its second application. The blocks will be denoted according to the range of contiguous sectors they interact with and, for the schemes that we shall refer to as type “T”, “V” and “W”, they generically comprise the six blocks: $\mathbf{M}_{[c:ne]}$, $\mathbf{M}_{[nne:n]}$, $\mathbf{M}_{[nnw:w]}$, $\mathbf{M}_{[wsw:sw]}$, $\mathbf{M}_{[ssw]}$, $\mathbf{M}_{[s:ese]}$. For the less symmetric family of schemes we shall refer to as “U”, only four blocks suffice: $\mathbf{M}_{[c:nne]}$, $\mathbf{M}_{[nnw:w]}$, $\mathbf{M}_{[wsw:ssw]}$, $\mathbf{M}_{[sse:ese]}$. When the stencil values are denoted by the column vector \mathbf{P} and the expansion coefficients by vector \mathbf{C} , the sequence of operators for these symmetrized stencils of the types we shall refer to as “T”, “V” and “W” is

$$\mathbf{C} = \mathbf{H}^T \mathbf{M} \mathbf{H} \mathbf{G} \mathbf{F} \mathbf{P}, \quad (3.1)$$

while, for the semi-symmetrized stencil of type “U” we shall use instead the simpler sequence:

$$\mathbf{C} = \mathbf{M} \mathbf{G} \mathbf{F} \mathbf{P}. \quad (3.2)$$

In each case, the computational work is dominated by multiplications and summations associated with the nonvanishing elements of the diagonal blocks of \mathbf{M} , and, as before, we shall continue to take the liberty of ignoring the cost of the sparse sums and differences, such as those associated with the operators \mathbf{F} , \mathbf{G} and \mathbf{H} . We provide a definition of the blocks of \mathbf{M} for the simplest members of these new families of schemes below; higher order versions are relatively easily obtained from the algebraic definitions we have provided by the obvious generalizations. In these symmetrized schemes, where the stencil is larger than is formally needed to derive only coefficients of total degree m , the vectors \mathbf{C} of expansion coefficients is correspondingly larger and therefore contains arguably superfluous terms, $x^i y^j$, with $i + j > m$. The selection of these additional terms is strictly in accordance with the unique identification we established in section 2 between a stencil point with alternating line labels i (for x_i) and j for y_j and the coefficient of the polynomial term in $x^i y^j$. Note, however, that the coordinate origin needs sometimes to be displaced by a half grid unit in order to collocate the new coordinate origin (for the Taylor series) with the center of symmetry of the symmetrized stencil. The pattern will be made clearer by consideration of the example stencils to follow.

(a) *Type T schemes, exemplified by T_4*

This stencil has 21 points and defines the expansion coefficients according to the \mathbf{M} blocks:

$$\mathbf{M}_{[c:ne]}^{(T_4)} = \begin{bmatrix} 1 & 0 & 0 & 0 & 0 \\ -\frac{5}{2} & \frac{2}{3} & -\frac{1}{24} & 0 & 0 \\ 6 & -2 & \frac{1}{2} & 0 & 0 \\ -12 & 7 & -1 & \frac{1}{2} & -4 \\ 6 & -\frac{19}{6} & \frac{1}{6} & -\frac{1}{12} & \frac{5}{3} \end{bmatrix}, \quad (3.3a)$$

$$\mathbf{M}_{[nne:n]}^{(T4)} = \begin{bmatrix} -\frac{1}{2} & 1 & -1 \\ 0 & \frac{2}{3} & -\frac{1}{24} \\ 0 & -2 & \frac{1}{2} \end{bmatrix}, \quad (3.3b)$$

$$\mathbf{M}_{[nnw:w]}^{(T4)} = \begin{bmatrix} -\frac{1}{4} & 1 & 0 & -\frac{3}{2} & 0 \\ \frac{1}{48} & -\frac{5}{12} & \frac{1}{24} & \frac{19}{24} & -\frac{1}{12} \\ 0 & \frac{1}{2} & -\frac{1}{4} & -1 & \frac{1}{2} \\ 0 & 0 & 0 & -\frac{1}{3} & \frac{1}{24} \\ 0 & 0 & 0 & \frac{1}{2} & -\frac{1}{4} \end{bmatrix}, \quad (3.3c)$$

$$\mathbf{M}_{[wsw:sw]}^{(T4)} = \begin{bmatrix} \frac{1}{8} & -\frac{1}{2} \\ -\frac{1}{24} & \frac{5}{12} \end{bmatrix}, \quad (3.3d)$$

$$\mathbf{M}_{[ssw]}^{(T4)} = \begin{bmatrix} 1 \\ 8 \end{bmatrix}, \quad (3.3e)$$

$$\mathbf{M}_{[s:ese]}^{(T4)} = \begin{bmatrix} -\frac{1}{3} & \frac{1}{24} & 0 & 0 & 0 \\ \frac{1}{2} & -\frac{1}{4} & 0 & 0 & 0 \\ -1 & \frac{1}{2} & -\frac{1}{4} & \frac{1}{2} & 0 \\ \frac{19}{24} & -\frac{1}{12} & \frac{1}{24} & \frac{5}{12} & \frac{1}{48} \\ -\frac{3}{2} & 0 & 0 & 1 & -\frac{1}{4} \end{bmatrix}. \quad (3.3f)$$

The vector of coefficients is partitioned according to the scheme:

$$\mathbf{C} = [C_{0,0}, C_{2,0}, C_{4,0}, C_{4,2}, C_{2,2} | C_{2,4}, C_{0,2}, C_{0,4} | C_{1,4}, C_{1,2}, C_{3,2}, C_{1,0}, C_{3,0} | C_{3,1}, C_{1,1} \\ | C_{1,3} | C_{0,1}, C_{0,3}, C_{2,3}, C_{2,1}, C_{4,1}]. \quad (3.4)$$

We note that elements of this vector include terms of total degree 5 and even 6.

The generalizations of this scheme's stencil to those of higher even orders is simply done by adding points all around no more than one grid unit away for each two-units increment of the formal order. The stencil sizes and the nominal computational costs of these even-order schemes are listed in columns "T" of the tables 2 and 3 respectively.

(b) *Type U schemes, exemplified by U4*

This stencil has 18 points and defines the expansion coefficients according to the \mathbf{M} blocks:

$$\mathbf{M}_{[c:nne]}^{(U4)} = \begin{bmatrix} \frac{75}{128} & -\frac{25}{256} & \frac{3}{256} & 0 & 0 & 0 \\ -\frac{17}{24} & \frac{13}{16} & -\frac{5}{48} & 0 & 0 & 0 \\ 1 & -\frac{3}{2} & \frac{1}{2} & 0 & 0 & 0 \\ 1 & -1 & 0 & \frac{1}{2} & -\frac{1}{2} & 0 \\ -\frac{11}{8} & \frac{1}{8} & 0 & -\frac{1}{16} & \frac{35}{48} & -\frac{1}{24} \\ 3 & 0 & 0 & 0 & -2 & \frac{1}{2} \end{bmatrix}, \quad (3.5a)$$

$$\mathbf{M}_{[nmw:w]}^{(U4)} = \begin{bmatrix} -\frac{35}{24} & -\frac{1}{12} & \frac{1}{24} & \frac{11}{4} & -\frac{1}{12} & 0 \\ 4 & -1 & 0 & -6 & 0 & 0 \\ 3 & 0 & -1 & -6 & 2 & 0 \\ 0 & 0 & 0 & -\frac{75}{64} & \frac{25}{384} & -\frac{3}{640} \\ 0 & 0 & 0 & \frac{17}{4} & -\frac{13}{8} & \frac{1}{8} \\ 0 & 0 & 0 & -10 & 5 & -1 \end{bmatrix}, \quad (3.5b)$$

$$\mathbf{M}_{[wsw:ssw]}^{(U4)} = \begin{bmatrix} \frac{1}{2} & -\frac{3}{2} & 0 \\ -\frac{1}{48} & \frac{35}{48} & -\frac{1}{12} \\ 0 & -1 & \frac{1}{2} \end{bmatrix}, \quad (3.5c)$$

$$\mathbf{M}_{[sse:ese]}^{(U4)} = \begin{bmatrix} -\frac{35}{96} & \frac{1}{24} & \frac{1}{32} \\ \frac{1}{2} & -\frac{1}{4} & 0 \\ \frac{1}{4} & 0 & -\frac{1}{4} \end{bmatrix}. \quad (3.5d)$$

The vector of coefficients is partitioned according to the scheme:

$$\mathbf{C} = [C_{0,0}, C_{2,0}, C_{4,0}, C_{2,2}, C_{0,2}, C_{0,4} | C_{1,2}, C_{1,4}, C_{3,2}, C_{1,0}, C_{3,0}, C_{5,0} \\ | C_{3,1}, C_{1,1}, C_{1,3} | C_{0,1}, C_{0,3}, C_{2,1}]. \quad (3.6)$$

Again, the generalizations to other even-ordered schemes is done in the obvious manner. The stencil sizes (Table 2) and computational costs (Table 3) are listed under the column heading ‘‘U’’.

(c) *Type V schemes, exemplified by V3*

This stencil has 13 points and defines the expansion coefficients according to the \mathbf{M} blocks:

$$\mathbf{M}_{[c:ne]}^{(V3)} = \begin{bmatrix} 1 & 0 & 0 & 0 \\ -\frac{5}{2} & \frac{2}{3} & -\frac{1}{24} & 0 \\ 6 & -2 & \frac{1}{2} & 0 \\ 4 & -2 & 0 & 1 \end{bmatrix}, \quad (3.7a)$$

$$\mathbf{M}_{[nne:n]}^{(V3)} = \begin{bmatrix} \frac{2}{3} & -\frac{1}{24} \\ -2 & \frac{1}{2} \end{bmatrix}, \quad (3.7b)$$

$$\mathbf{M}_{[nnw:w]}^{(V3)} = \begin{bmatrix} -\frac{1}{4} & \frac{1}{2} & 0 \\ 0 & -\frac{1}{3} & \frac{1}{24} \\ 0 & \frac{1}{2} & -\frac{1}{4} \end{bmatrix}, \quad (3.7c)$$

$$\mathbf{M}_{[wsw:sw]}^{(V3)} = \begin{bmatrix} \frac{1}{4} \end{bmatrix}, \quad (3.7d)$$

$$\mathbf{M}_{[s:ese]}^{(V3)} = \begin{bmatrix} -\frac{1}{3} & \frac{1}{24} & 0 \\ \frac{1}{2} & -\frac{1}{4} & 0 \\ \frac{1}{2} & 0 & -\frac{1}{4} \end{bmatrix}. \quad (3.7e)$$

The vector of coefficients is partitioned according to the scheme:

$$\mathbf{C} = [C_{0,0}, C_{2,0}, C_{4,0}, C_{2,2} | C_{0,2}, C_{0,4} | C_{1,2}, C_{1,0}, C_{3,0} | C_{1,1} | C_{0,1}, C_{0,3}, C_{2,1}]. \quad (3.8)$$

These schemes generalize only to odd-order schemes and, as before, are obtained incrementally by adding to the existing stencil only new points that are no more than a single grid unit away all around. The sizes and costs of these schemes are given in the table 2 and 3 columns headed “V”

(d) *Type W schemes, exemplified by W3*

This stencil has 12 points and defines the expansion coefficients according to the \mathbf{M} blocks:

$$\mathbf{M}_{[c:ne]}^{(W3)} = \begin{bmatrix} \frac{1}{8} & -\frac{1}{4} \\ -\frac{1}{32} & \frac{5}{16} \end{bmatrix}, \quad (3.9a)$$

$$\mathbf{M}_{[nne:n]}^{(W3)} = \begin{bmatrix} \frac{1}{8} \end{bmatrix}, \quad (3.9b)$$

$$\mathbf{M}_{[nnw:w]}^{(W3)} = \begin{bmatrix} -\frac{1}{4} & \frac{1}{4} & 0 \\ \frac{1}{32} & -\frac{5}{16} & \frac{1}{96} \\ 0 & \frac{3}{4} & -\frac{1}{4} \end{bmatrix}, \quad (3.9c)$$

$$\mathbf{M}_{[wsw:sw]}^{(W3)} = \begin{bmatrix} \frac{1}{2} & -3, \\ -\frac{1}{24} & \frac{5}{4} \end{bmatrix}, \quad (3.9d)$$

$$\mathbf{M}_{[ssw]}^{(W3)} = \begin{bmatrix} \frac{1}{2} \end{bmatrix}, \quad (3.9e)$$

$$\mathbf{M}_{[s:ese]}^{(W3)} = \begin{bmatrix} -\frac{1}{4} & \frac{3}{4} & 0, \\ \frac{1}{96} & -\frac{5}{16} & \frac{1}{32}, \\ 0 & \frac{1}{4} & -\frac{1}{4} \end{bmatrix}. \quad (3.9f)$$

The vector of coefficients is partitioned according to the scheme:

$$\mathbf{C} = [C_{2,0}, C_{0,0} | C_{0,2} | C_{1,2}, C_{1,0}, C_{3,0} | C_{3,1}, C_{1,1} | C_{1,3} | C_{0,3}, C_{0,1}, C_{2,1}]. \quad (3.10)$$

Stencil sizes of the odd-order generalizations are given in Table 2 and computational costs are listed in Table 3 under the heading “W”.

(e) *Non-collocating interpolations*

In all the symmetrized diamond stencil schemes, types “T”, “U”, “V” and “W” the coefficient vectors contain a few coefficients associated with a polynomial term of total degree exceeding the nominal order m for that scheme. Obviously, there is a computational advantage to be gained by discarding, i.e., *not* calculating, those superfluous coefficients. The computational saving for doing this can be considerable, especially as the order m becomes large, as we see in the columns of Table 3 that are marked with an asterisk. However, there is downside to doing this, which is that the reconstructed polynomial values are no longer collocated with sampled values at the stencil points. This may prove disadvantageous in many applications since collocating provides a valuable degree of effective control over the way the interpolating polynomial can vary within the span of the stencil in practice.

(f) *Cartesian product schemes*

In many ways the simplest array from which to extract high-order interpolating Taylor coefficients is a sub-square of the grid. With $m + 1$ points in both cartesian directions, all partial derivatives, $C_{i,j}$ with $i \leq m$ and with $j \leq m$ and without further restriction, can be evaluated in the obvious sequence of two steps, x followed by y . But it is still worth invoking the symmetry reflection symmetries in x and y when doing this. The costs for evaluating all $(m + 1)^2$ available coefficients is given in Table 3 under column “C”; if we discard the superfluous terms of total degree exceeding m in the second step, we reduce the costs considerably to those shown under the heading “C*”.

(g) *Remarks*

It might be supposed that other configurations that would seem to qualify as symmetrized diamond stencils with fewer stencil points (for a given order m) could also compete with those we have designated “T” and “U” (even m schemes) or “V” and “W” (odd m schemes) but a

TABLE 2. STENCIL SIZES FOR THE STANDARD “DIAMOND” SCHEME (S), ITS SYMMETRIZED VARIANTS OF TYPE T, U (EVEN DEGREES ONLY), V AND W (ODD DEGREES ONLY), AND THE CARTESIAN-PRODUCT STENCIL (C) UP TO DEGREE $m = 16$.

m	S	T	U	V	W	C
2	6					9
3	10			13	12	16
4	15	21	18			25
5	21			25	24	36
6	28	37	32			49
7	36			41	40	64
8	45	57	50			81
9	55			61	60	100
10	66	81	72			121
11	78			85	84	144
12	91	109	98			169
13	105			113	112	196
14	120	141	128			225
15	136			145	144	256
16	153	177	162			289

closer examination reveals such schemes to be, like the stencil of Fig. 2(b), in violation of the gap-free monotonicity rules we discussed in section 2. The trends in the behavior of the valid symmetrized schemes as m increases and their comparison with the cartesian scheme “C” and the standard (unsymmetrized) diamond scheme, “S”, can be seen more easily in graphical form. The data of Table 3 are therefore plotted as graphs using a log-log scale in Figs. 6–9. Here it is clear to see that the standard schemes “S”, while at least competitive with the symmetrized collocating schemes compared in Figs. 6 and 8 at the very lowest odd and even orders, cannot be justified at higher orders m , and especially not when the requirement for collocation is relaxed (Figs. 7 and 9). As the order m increases, the “T” and the “V” configurations emerge as the most efficient schemes of even and odd order respectively, although there are indications that, somewhat beyond the largest orders m we have been able to investigate here, the cartesian product schemes “C” might eventually enjoy computational superiority.

4. DISCUSSION

When it is necessary to extract from a grid the horizontal coefficients of an approximating polynomial in an efficient manner we find that, especially as the intended order increases, it is advantageous to exploit whatever symmetries the sampling stencil provides. The smallest and most compact stencils are the standard “diamond” stencils (Purser 2007) so, when the Taylor coefficients are needed at many vertical levels but at the same horizontal target location, there

TABLE 3. NOMINAL EVALUATION COSTS, AS MEASURED BY MATRIX OCCUPANCY, FOR THE VARIOUS STENCILS OF TABLE 1. THESE ARE THE STANDARD “DIAMOND” SCHEME (S), ITS SYMMETRIZED VARIANTS OF TYPE T, U (EVEN DEGREES ONLY), V AND W (ODD DEGREES ONLY), AND THE CARTESIAN-PRODUCT STENCIL (C) UP TO DEGREE $m = 16$. FOR THE SCHEMES WITH ASTERISKS, THE SUPERFLUOUS TAYLOR SERIES TERMS OF TOTAL DEGREE EXCEEDING m ARE NOT EVALUATED, REDUCING THE EFFECTIVE COUNT ON MATRIX OCCUPANCY AND HENCE THE ESTIMATED COST.

m	S	T	T*	U	U*	V	V*	W	W*	C	C*
3	30					27	19	24	21	64	52
4	56	61	39	56	46					100	74
5	183					82	67	88	80	216	171
6	292	177	127	164	144					294	219
7	467					206	179	232	217	512	400
8	658	404	313	390	355					648	484
9	990					441	399	512	485	1000	775
10	1346	805	654	802	746					1210	905
11	1864					850	786	988	946	1728	1332
12	2374	1446	1217	1484	1400					2028	1518
13	3190					1499	1409	1734	1670	2744	2107
14	4008	2418	2086	2535	2415					3150	2359
15	5146					2479	2354	2841	2751	4096	3136
16	6210	3795	3337	4328	4129					4624	3464

is no more efficient strategy than to base the extraction on the appropriate linear relationship between the coefficients and the sampled points of the diamond stencil at each level, since the set of weights in the formula are the same at each level. In addition to exploiting the bilateral reflection symmetry of the diamond stencils, there is a further advantage to be obtained, at the higher orders of expansion at least) from applying linear transformations associated with successive line-differential operators along the available lines of the stencil parallel and perpendicular to the symmetry axis. When a high-order Taylor expansion is needed on a single horizontal surface, the computational cost of evaluating the coefficients is significantly reduced by augmenting the diamond stencils in ways that add additional symmetries. For the coefficients of a collocation polynomial the optimal symmetrization may differ from the one that is optimal when the higher-than-nominal degree coefficients are discarded. For even orders, the symmetrization schemes of type U are better than those of type T up about 10th order when all terms are retained, but the T schemes are better at all orders when the higher degree terms are discarded from the computation (so that the implied polynomial no longer exactly fits the sample values). For the odd-order schemes, only the collocating scheme W3 beats the corresponding V scheme; in all other cases, whether the superfluous higher order terms are discarded or not, the V schemes are better than the corresponding W schemes. Another possible stencil at each order is the cartesian product “square” stencil of $(m + 1)^2$ points, but this has been shown to be inefficient until very high orders of accuracy are demanded.

REFERENCES

Evaluation costs for Taylor series of odd degree
 Diamond stencils compared with symmetrized stencils
 without discarding any evaluated terms

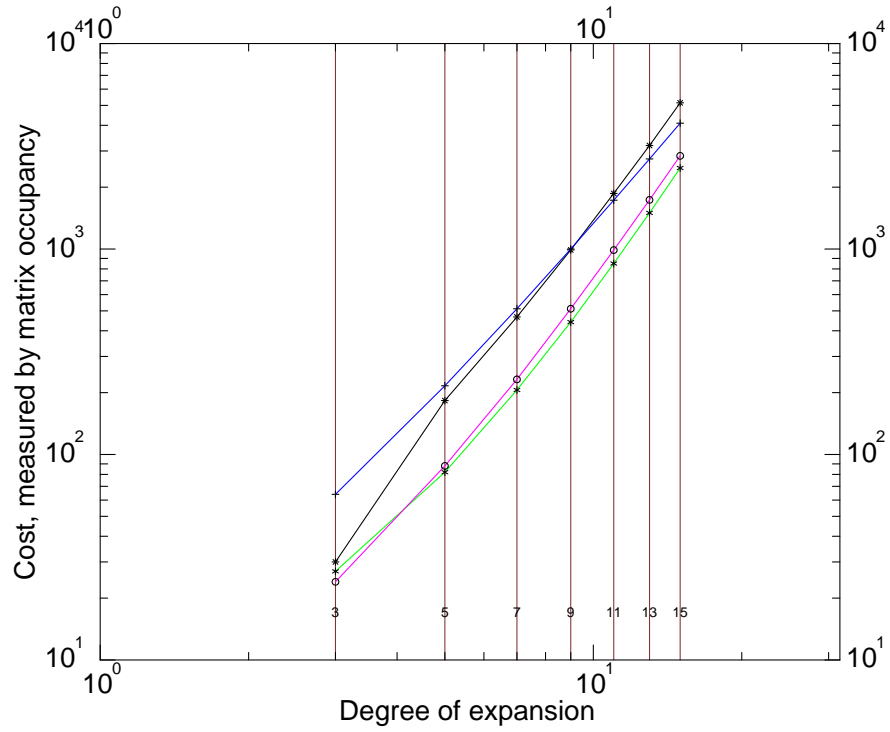


Figure 6. Computational costs approximated by the number of “multiply” operations needed to compute the Taylor coefficients accommodated by the odd-order stencils of types “S” (black), “V” (green); “W” (red) and the cartesian product stencil, “C” (blue) at orders m up to 15.

Purser, R. J.

2007 Diamond interpolation: a class of accurate compact-stencil grid interpolation methods. NOAA/NCEP Office Note 454, 13 pp.

Evaluation costs for Taylor series of odd degree
 Diamond stencils compared with symmetrized stencils
 but without computing the unwanted terms of excessive total degree

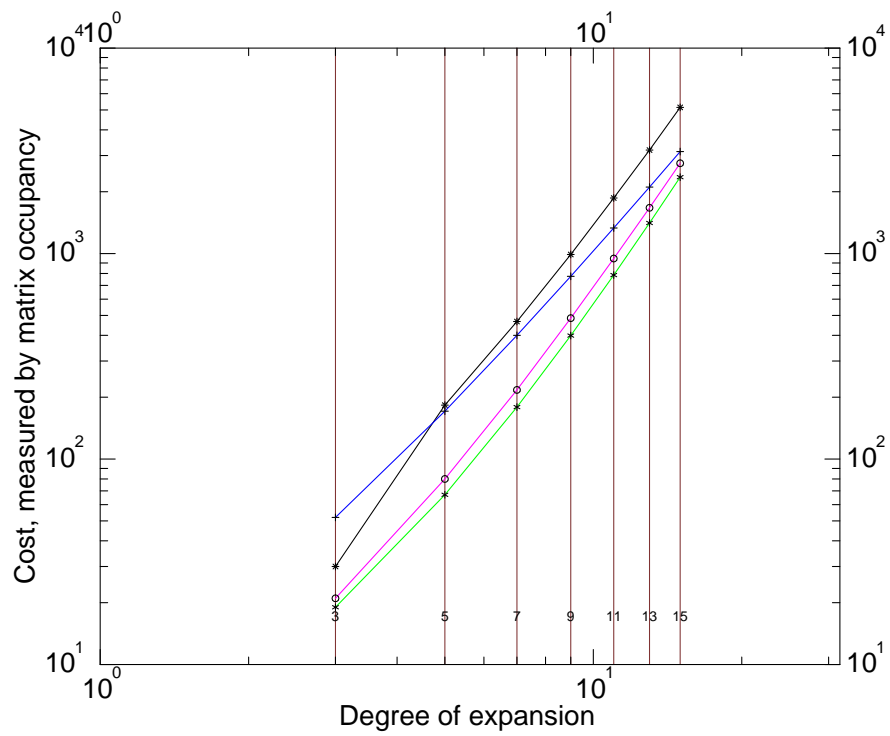


Figure 7. Like Fig. 6 but discarding terms of total degree greater than m

Evaluation costs for Taylor series of even degree
 Diamond stencils compared with symmetrized stencils
 without discarding any evaluated terms

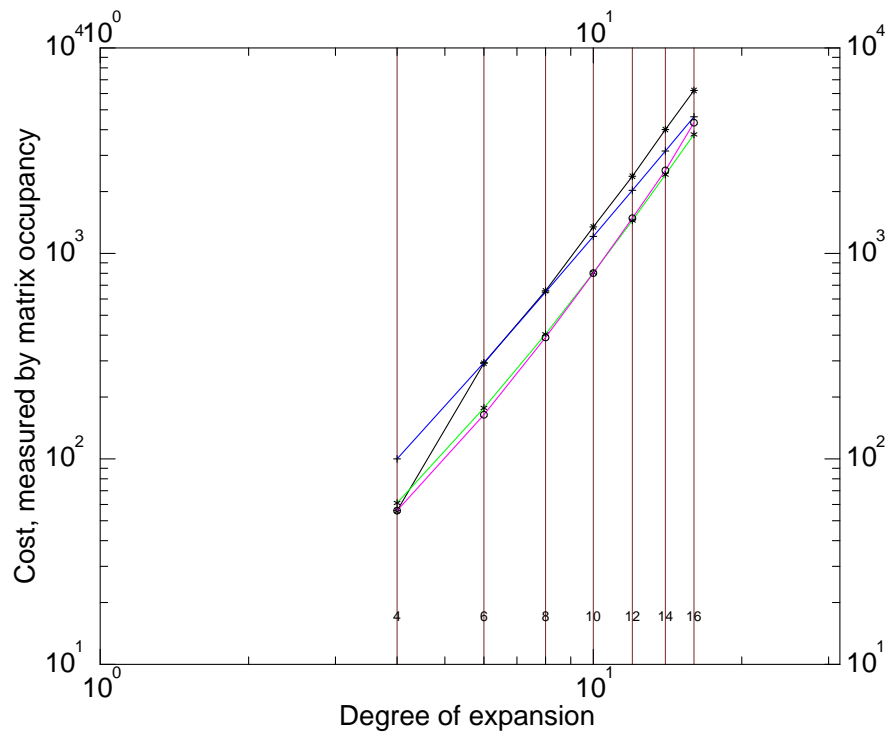


Figure 8. Like Fig. 6 but comparing even-order schemes “S” (black), “T” (green), “U” (red) and “C” (blue) for orders m up to 16.

Evaluation costs for Taylor series of even degree
 Diamond stencils compared with symmetrized stencils
 but without computing the unwanted terms of excessive total degree

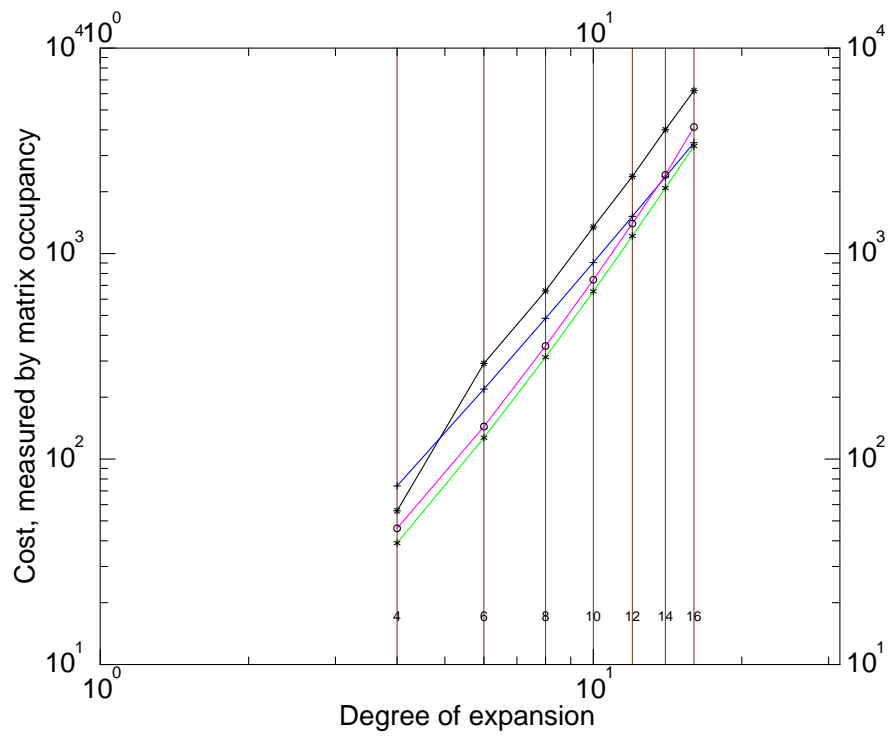


Figure 9. Like Fig. 8 but discarding all the superfluous terms of total degree exceeding the nominal degree m